Eur. Phys. J. B **15**, 35–40 (2000)

THE EUROPEAN PHYSICAL JOURNAL B

EDP Sciences

Neutron scattering study of transverse magnetism in the metamagnet $FeBr_2$

Ch. Binek[1,a], T. Kato[1,b], W. Kleemann[1], O. Petracic[1], D. Bertrand[2], F. Bourdarot[3], P. Burlet[3], H. Aruga Katori[4], K. Katsumata[4], K. Prokes[5,c], and S. Welzel[5]

[1] Laboratorium für Angewandte Physik, Gerhard-Mercator-Universität, 47048 Duisburg, Germany
[2] Laboratoire de Physique des Solides, INSA, 31077 Toulouse Cedex, France
[3] Institut Laue Langevin (ILL), 38042 Grenoble Cedex 9, France
[4] The Institute of Physical and Chemical Research (RIKEN), Wako, Saitama 351-01, Japan
[5] Hahn-Meitner-Institut (HMI), 14109 Berlin, Germany

Received 27 September 1999 and Received in final form 6 December 1999

Abstract. In order to clarify the nature of the additional phase transition at $H_1(T) < H_c(T)$ of the layered antiferromagnetic (AF) insulator $FeBr_2$ as found by Aruga Katori *et al.* (1996) we measured the intensity of different Bragg-peaks in different scattering geometries. Transverse AF ordering is observed in both AF phases, AF I and AF II. Its order parameter exhibits a peak at $T_1 = T(H_1)$ in temperature scans and does not vanish in zero field. Possible origins of the step-like increase of the transverse ferromagnetic ordering induced by a weak in-plane field component when entering AF I below T_1 are discussed.

PACS. 75.25.+z Spin arrangements in magnetically ordered materials (including neutron and spin-polarized electron studies, synchrotron-source X-ray scattering, etc.) – 75.30.Kz Magnetic phase boundaries (including magnetic transitions, metamagnetism, etc.) – 75.50.Ee Antiferromagnetics

1 Introduction

Metamagnets with large uniaxial anisotropy like $FeCl_2$ and $FeBr_2$ are widely accepted as model systems for investigating fundamental properties of antiferromagnets. Both compounds are ionic insulators with localized magnetic moments at the Fe^{2+}-sites, arranged in triangular layers. The inset of Figure 1 shows the hexagonal unit cell of $FeBr_2$ (space group $D^3_{3d} = P\bar{3}m1$, Néel temperature $T_N = 14.1$ K), where adjacent (001) layers of Fe^{2+} ions are separated by two layers of Br^- ions. The spin directions at low temperatures, $T \ll T_N$, and in zero external magnetic field, H, are conventionally assumed to point parallel and antiparallel to [001], respectively, from layer to layer. Thus a Néel type ground state with "up" and "down" spin sublattices seems to emerge as in the case of $FeCl_2$ (space group $D^5_{3d} = R\bar{3}m$, $T_N = 23.7$ K). However, while $FeCl_2$ – when exposed to an axial magnetic field H – reveals a classic tricritical point on its H-T phase line [1,2], $FeBr_2$ behaves in a more complicated fashion (Fig. 1).

Similarly as in $FeCl_2$ the lines H_{c1} and H_{c2} denote the phase transition of first-order from AF long-range order to the paramagnetic (PM) saturated phase *via* a mixed phase (AF+PM). However, above the multicritical point (MCP) temperature, $T_{MCP} = 4.6$ K, apart from the critical phase line, $H_c(T)$, regions of strong non-critical fluctuations are encountered. They are peaking along novel lines denoted as $H_-(T)$ and $H_+(T)$, respectively [3]. Between H_- and H_+ the hyperfine field acting on the down-spin sublattice gradually varies from extreme negative to positive values, thus indicating strong transverse spin precession on the Mössbauer spectroscopic time scale [4]. In addition, another line, $H_1(T)$, is observed in the vicinity of $H_-(T)$. It was discovered by Aruga Katori *et al.* [5] in specific heat data and depicts a hitherto unexpected first-order phase transition. In magnetization measurements, using magnetic fields tilted with respect to the layer normal, it manifests itself as a slightly shifted line, $H_1'(T)$ [6].

Recently, attention has been focused on the investigation of the nature of the phase transition at $H_1(T)$. It divides the AF phase region into two sub-phases AF I ($H < H_1$) and AF II ($H_1 < H < H_c$). From magnetization measurements in tilted fields [6] it was conjectured that transverse spin ordering exists in the AF II phase, with a jump of the axial magnetization component $M_{ax} = M_z$ at $H_1'(T)$, provided that the transverse (*i.e.* in-plane) magnetization, M_{pl}, is aligned by an auxiliary field, H_{pl}. In order

[a] e-mail: binek@kleemann.uni-duisburg.de
[b] On leave of absence from the Department of Physics, Tokyo Institute of Technology, Japan
[c] On leave of absence from the Department of Electronic Structures, Charles University, Prague, Czech Republic

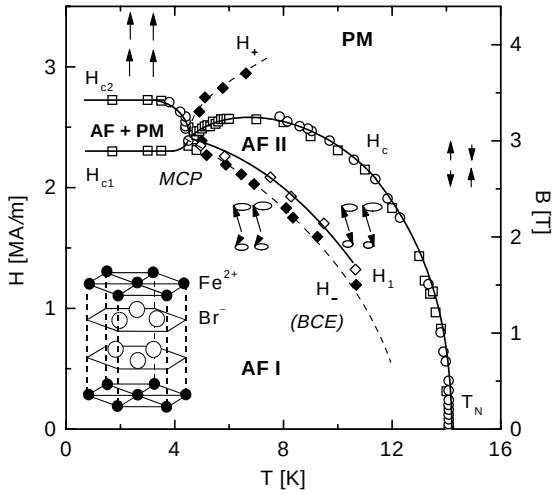

Fig. 1. H-T (B-T) phase diagram of $FeBr_2$ presented by interpolated lines and data points [3,6], where H ($B = \mu_0 H$) is the applied axial magnetic field (induction). H_c is the second-order phase line, while H_{c1} and H_{c2} are the boundaries of the mixed phase AF + PM. Dashed lines H_- and H_+ denote the peak positions of the non-critical fluctuations, while H_1 emerges from specific heat [5] measurements [6] in axial fields. Critical points (MCP and BCE) and temperatures (T_N), and phases (PM, AF I and AF II) are indicated (see text). Tentative spin structures are schematically sketched by arrows and precession circles of their tips in oblique phases. They refer to the layered lattice structure as depicted by the unit cell in the inset (see text).

to explain the obvious coupling between the in- and out-of-plane spin polarization an off-diagonal exchange interaction between planar and axial spin components was postulated, which is allowed in trigonal point symmetry [7].

Within the framework of a simple Néel state model with rigid spins the discontinuous enhancement of the ferromagnetic (FM) order parameter should give rise to a reverse jump in the AF order parameter. However, this was not clearly confirmed by elastic neutron scattering measurements. Apart from criticality at the phase boundary, $H_c(T)$, and non-critical fluctuations at H_+ and H_-, only a weak anomaly of the axial AF order parameter is evidenced at $H_1(T)$ by virtue of the temperature and magnetic field dependencies of the (2, 0, 1/2) neutron scattering intensities when scaled with $T_c(H)$ or $T_1(H)$ [8]. Thus, in order to solve the enigmatic situation and to clarify the characteristics of $H_1(T)$ it appears useful to investigate more carefully the spin structure, *viz.* in particular the planar components of the AF order parameter. To this end novel experiments of neutron scattering with magnetic fields both parallel and tilted to the c axis have been done. For the first time they evidence that the ground state spin configuration of $FeBr_2$ in zero external field exhibits a transverse component of the AF order parameter in all AF phases, *i.e.* at $H < H_c, H_{c1}$. As a signature of the phase transition at $H_1(T)$ it shows a peak together with a step-like rise of the transverse FM moment in the tilted configuration.

2 Experimental details

Neutron scattering measurements were performed at the High Flux Reactor at the Institut Laue Langevin (ILL) in Grenoble, France, and at the Berlin Neutron Scattering Center of the Hahn-Meitner Institut (HMI) in Berlin, Germany.

In the ILL experiments we used the D15-instrument as a two-axis thermal neutron normal-beam diffractometer with a cryostat containing a vertical superconducting magnet ($\mu_0 H \leq 6$ T). The neutron wavelength was $\lambda = 1.176$ Å with a $\lambda/2$ contamination of about 0.1%. It should be remarked that a non-horizontal scattering plane was chosen in some experiments. In those cases we changed the detector tilt angle, ν, for the different Bragg peaks. Almost all data shown in this paper are obtained from omega scans. We used two $FeBr_2$ samples with sizes $20 \times 15 \times 10$ mm^3 and $4 \times 6 \times 5$ mm^3, mounted either with the c axis parallel to the applied field or tilted under an angle $\theta \approx 30°$ with respect to the field axis. Magnetization measurements show that for angles $\theta \leq 30°$ the tilting has only a small influence on the phase transition at $H_c(T)$. It seems that only the component $H\cos(\theta)$ drives the global critical behavior [6].

At HMI we used the E4-instrument employing a sample with size $6 \times 6 \times 2$ mm^3. It was mounted with its c axis parallel to the applied field, $\mu_0 H \leq 6$ T, which was supplied by a horizontal superconducting magnet. In this configuration it was straightforward to measure the (0, 0, 1/2) Bragg reflection, where both the c and the field axis lay in the scattering plane. The neutron wavelength was $\lambda = 2.4$ Å with the collimator condition "40′-40′-open-40′′".

Magnetization and ac susceptibility data were obtained using a SQUID magnetometer (Quantum Design MPMS5S).

3 Experimental results

3.1 Scattering data from ILL

Figure 2 shows the measurements of the scattering intensity I *vs.* temperature T for the (2, 0, 1/2) Bragg peak, which is a measure of the axial AF order parameter. The c axis is parallel to the applied field, H, which is varied from $H = 0$ (curve 1) to $H = 2.39$ MA/m (curve 5). Two features are obvious: In agreement with previous work [8] the phase transitions at $T_c(H)$ are clearly indicated by points of inflexion in $I(T)$ (arrows) in accordance with those found in the magnetization curves, $M(T)$, two of which are shown in Figure 2 for $H = 1.91$ MA/m (curve 3′) and 2.39 MA/m (curve 5′). Furthermore the anomalous decrease of the intensity due to non-critical fluctuations is observed at $H_-(T)$, where the spin-down sublattice switches into an almost non-magnetized state, while the spin-up sublattice remains highly magnetized along the applied field. This causes an anomalous increase of M *vs.* T and a reduction of the AF order parameter

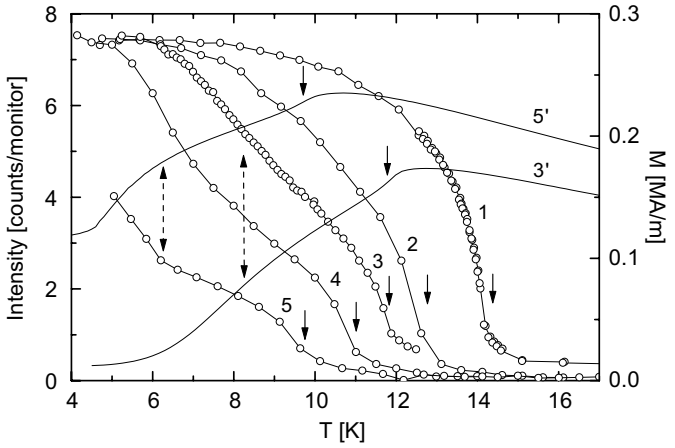

Fig. 2. Temperature dependence of scattering intensities (open circles, lefthand scale of count rates normalized with respect to the monitor value of the incident flux) at the antiferromagnetic Bragg peak (2, 0, 1/2) and magnetization of $FeBr_2$ (solid lines, righthand scale) for different axial fields, $H = 0$ (1), 1.59 (2), 1.91 (3, 3′), 2.15 (4) and 2.39 MA/m (5, 5′). Solid arrows denote the critical temperatures $T_c(H)$, while broken double arrows indicate the peak positions of non-critical fluctuations.

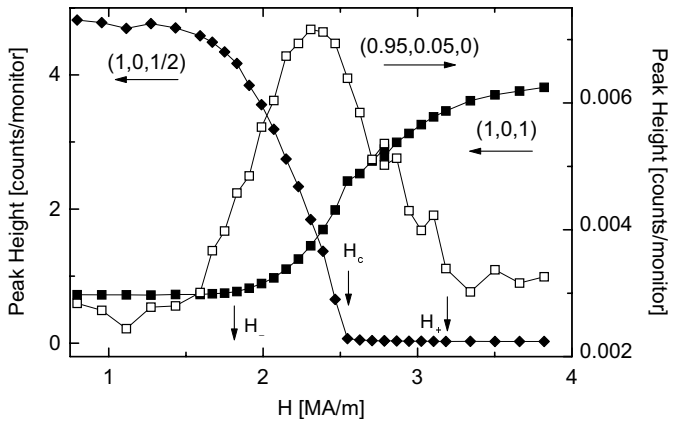

Fig. 3. Axial magnetic field dependence of scattering intensities (peak heights) at Bragg and off-Bragg positions (1, 0, 1/2), (1, 0, 1) and (0.95, 0.05, 0), respectively, at $T = 8.0$ K. The fields H_c, H_+ and H_- (see Fig. 1) are indicated by arrows.

as indicated by double arrows connecting the curves 3, 3′ and 5, 5′ in Figure 2, respectively. These features are also found in Monte Carlo simulations of Ising-type AF systems [9–11]. The non-critical fluctuations are typical of the axial system and are also observed as broad shoulders in the susceptibility, χ' [3], or in the specific heat, $c_{\rm mag}$ [5].

In Figure 3 the scattering peak intensity data of field sweeps at $T = 8$ K are shown. While the AF Bragg intensity, I (1, 0, 1/2), vanishes for increasing H at the critical value $H_c = 2.55$ MA/m (arrow), the intensity of the FM (1, 0, 0) Bragg peak increases like $M^2(H)$ [3]. As expected, it shows an inflection point at $H = H_c$. We also measured the off-Bragg peak scattering intensity near the (1, 0, 0) Bragg reflection at $(h, k, l) = (0.95, 0.05, 0)$, which is a measure of FM susceptibility or short range correlations. It peaks at $H \approx 2.31$ MA/m, a value lying between

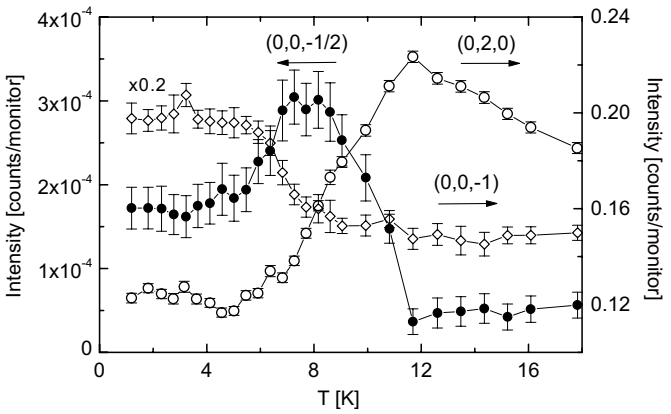

Fig. 4. Temperature dependence of scattering intensities measured in an applied magnetic field $H = 2.39$ MA/m (axial field component $H_{\rm ax} = H\cos(30°) \approx 2.07$ MA/m) at the Bragg peaks (0, 2, 0), (0, 0, −1) and (0, 0, −1/2), which represent the axial and transverse FM, and the transverse AF order, respectively. Note the multiplication of the (0, 0, −1) curve by a factor of 0.2.

$H_1 = 1.99$ MA/m and $H_c = 2.55$ MA/m, *i.e.* amidst (and thus probably characteristic of) the AF II region.

From this results it is concluded that the additional phase transition at $H_1(T)$ cannot be seen in axial fields *via* axial AF or FM Bragg intensities. It seemed, hence, advisable to measure a purely transverse Bragg peak, *e.g.* (0, 0, 1/2), which reflects AF ordering along the c axis, where the magnetization components lie orthogonally to the c axis. It has to be noticed that secondary order parameters like strain couple to bilinear correlation functions of the spin components, *e.g.* $\langle S_x^2 \rangle$. Unlike $\langle S_x \rangle$ they are, hence, not expected to reveal period-doubling along [001] and will not contribute to I $(0, 0, \pm 1/2)$. In order to detect this peak, we had to tilt the sample by 30° with respect to the field direction, being vertical in the case of the experiments at ILL. The same angle was also used in our previous magnetization measurements [6]. In this configuration we measured the intensities of the (0, 0, −1/2), (0, 0, −1) and (0, 2, 0) peaks.

Figure 4 shows the data obtained for the applied field $H = 2.39$ MA/m. The axial FM intensity of the (0, 2, 0) peak has a similar shape as the magnetization data. However, the transverse AF intensity as observed from the (0, 0, −1/2) peak reveals new information about the ordering of the spin components orthogonal to the c axis. For decreasing temperature we see a strong increase of the transverse AF ordering starting at $T \approx 11.7$ K. At $T \approx 8$ K it reaches a maximum and then decreases to a saturation value of about half of the peak value. It should be noticed that the axial field, which is responsible for the global critical behavior, is $H_{\rm ax} = H\cos(30°) \approx 2.07$ MA/m. Comparison with the phase diagram (Fig. 1) shows, that the corresponding value of the critical temperature, $T_c = 11.5$ K, is well reproduced. Consequently the additional phase transition at $H_1'(T)$ should occur at $T \approx 8$ K. Remarkably, in our measurement we find a maximum at this position. Moreover, at this value the transverse FM order

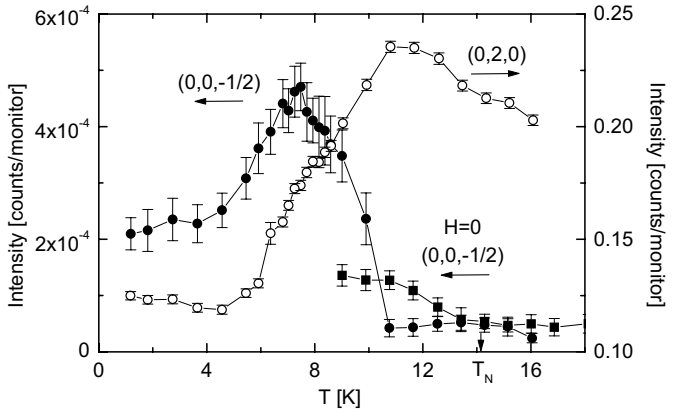

Fig. 5. Temperature dependence of scattering intensities measured in an applied magnetic field $H = 2.55$ MA/m (axial field component $H_{\rm ax} = H\cos(30^\circ) \approx 2.21$ MA/m) at the Bragg peaks (0, 2, 0) and (0, 0, $-1/2$) representing axial FM and planar AF order, respectively. The intensity of the (0, 0, $-1/2$) peak at $H = 0$ is denoted by solid squares. $T_{\rm N}$ indicates the Néel temperature.

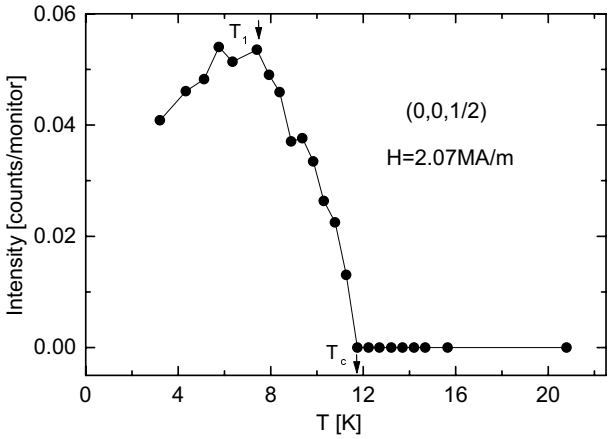

Fig. 6. Temperature dependence of scattering intensities measured in an applied axial magnetic field $H = 2.07$ MA/m at the Bragg peak (0, 0, 1/2) representing planar AF order. The data refer to omega scans deconvoluted into eight Gaussians (see text).

parameter, as seen in the (0, 0, -1) Bragg peak intensity, shows a step from a high saturation value at low temperatures to lower values at higher temperatures, $T > 8$ K. Near $T_{\rm c}$, at $T \approx 12$ K, another small step towards a lower saturation value is observed.

Similar features of the transverse AF order are found for a higher field value, $H = 2.55$ MA/m, as shown in Figure 5. Again the transverse AF order increases rapidly below the critical temperature, $T_{\rm c} = 10.7$ K, reaches a sharp maximum at $T = 7.5$ K and decreases upon further cooling to saturate at a scattering intensity $I \approx 0.44\ I(7.5\ {\rm K})$. Taking into account the value of the axial field in this case, $H_{\rm ax} = 2.55\ {\rm MA/m} \cdot \cos(30^\circ) \approx 2.2$ MA/m, and considering the phase diagram (Fig. 1) we should expect the additional phase transition at $T(H_1) = 7.5$ K in agreement with the position of the (0, 0, $-1/2$) peak intensity.

From the above measurements it is evident that transverse AF ordering occurs at all temperatures $T < T_{\rm c}(H)$. Interestingly, this assertion seems to hold even in zero external field. Figure 5 also shows $I(0, 0, -1/2)$ *vs.* T for $H = 0$ (solid squares), where a net increase $\delta I(0, 0, -1/2)$ is observed beyond errors when cooling to below $T_{\rm N} = 14.1$ K.

3.2 Scattering data from HMI

In contrast with the measurements done at ILL the c axis of the crystal was oriented parallel to the magnetic field in the HMI experiments. Thus within a possible error of less than 5° due to misalignment no in-plane field was present. Figure 6 shows I *vs.* T for the (0, 0, 1/2) Bragg peak for applied fields $H = H_{\rm ax} = 2.07$ MA/m. After removing the non-magnetic background as revealed by the bias values at $T \approx 20$ K, the data behave similarly as the curves obtained at ILL in Figures 4 and 5. The peak at $T_1(H)$ is lacking in low-fields ($H \leq 1.6$ MA/m, not shown), where only a step-like increase of the intensity is encountered at $T_{\rm c}(H)$ when cooling from high temperatures. This observation corroborates the idea of a bicritical endpoint terminating the phase line $H_1(T)$ at finite field values (BCE in Fig. 1).

It should be mentioned that the data presented in Figure 6 have been subtracted from a considerable background intensity and are weak and quite noisy. They refer to omega scans around the (0, 0, 1/2) Bragg peak exhibiting broad multi-peak structures of width $\delta\omega \approx \pm 2^\circ$. The data presented in Figure 6 refer to a decomposition of the omega curves into eight distinct Gaussian ones. In this situation it might be argued that an inhomogeneous field distribution across the sample might give rise to the observed secondary peaks. However, while such effects will be harmful when determining magnetic phase boundaries [12, 13], they are not expected to modify Bragg reflection conditions apart from higher order coupling phenomena (*e.g.* magnetoelastic distortions). In order to exclude this possibility we have ascertained that nuclear Bragg peaks as measured even at $T > T_{\rm N}$ reveal the same multi-peaked structure of the omega scans. That is why we are convinced that the sample quality obviously suffered from considerable mosaicity (textured polycrystallinity).

Figure 7 shows the peak height of the (0, 0, 1/2) Bragg peak *vs.* field for two temperatures, $T = 1.8$ and 7.8 K. Within errors, one can conclude, that I (0, 0, 1/2) starts with a plateau at low fields (even at zero field). In the curve for $T = 1.8$ K (open circles) one observes a slight increase upon reaching the lower boundary of the mixed phase ($H_{\rm c1} = 2.35$ MA/m, see Fig. 1), then a strong decrease in the mixed phase, and finally saturation above $H_{\rm c2} = 2.75$ MA/m (arrows). This corresponds well with the phase diagram of $FeBr_2$ (Fig. 1). The second curve, for $T = 7.8$ K (solid circles) shows a similar behavior, but a smoother decrease. It starts in the vicinity of $H_1(8\ {\rm K}) \approx 2.0$ MA/m (arrow) and levels off at $H_{\rm c}(8\ {\rm K}) \approx 2.6$ MA/m. Hence, the transverse AF order parameter clearly decreases in both the mixed AF + PM and the AF II phase.

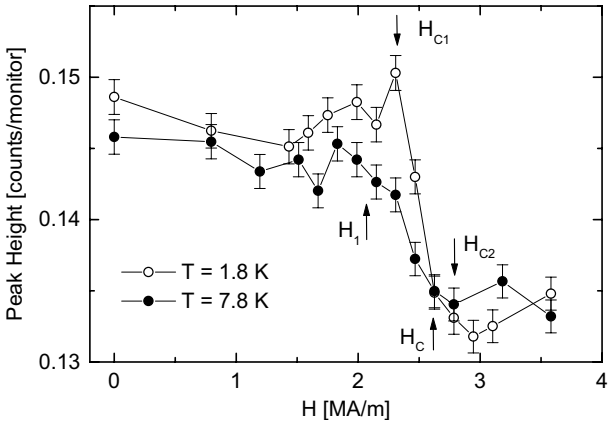

Fig. 7. Axial magnetic field dependence of the Bragg peak height at (0, 0, 1/2) for $T = 1.8$ (open circles) and 7.8 K (solid circles). The fields H_c, H_1, H_{c1} and H_{c2} (see Fig. 1) are indicated by arrows.

4 Discussion

The (0, 0, 1/2) Bragg peak intensity data reveal new information about the magnetic ordering in $FeBr_2$. We believe that Figure 4 is particularly crucial for the interpretation of the data.

First, from the present data we conclude that non-vanishing transverse spin-components do exist and, hence, AF transverse spin ordering is encountered in $FeBr_2$. It seems to disappear only beyond the critical line, $H_c(T)$, and vanishes as $T \to T_c(H)$ in a similar way as does the longitudinal AF order parameter (Fig. 2). Unexpected and contrasting with our previous interpretation [6], it is now certain that non-vanishing AF transverse spin order does exist both at low temperatures and in weak fields. This seems to be true even for zero-field (Figs. 5 and 6), and means, that the ground-state of $FeBr_2$ must be an oblique spin state. The corresponding spin structure expected for the AF II phase is qualitatively depicted in Figure 1 by antiparallel oblique arrows and precession circles of their tips. The field-induced magnetization is taken into account by different lengths of the arrows on the up- and down-spin sublattices, respectively.

Second, as is evident from the temperature scans of Figures 4 and 5, the transverse AF order parameter has a maximum at the additional phase transition line, $T_1 = T(H_1)$. It decreases upon cooling and attains a constant value, $I_{\min} \approx 0.5 I_{\max}$, at low T. This curve profile was found both in the ILL data with $H_{\rm pl} \neq 0$ and in the HMI data with $H_{\rm pl} \approx 0$.

Third, in the AF II phase at $T > T_1$ we observe an abrupt destruction of the transverse FM order at increasing temperatures (concave curvature I *vs.* T), while the transverse AF order decays smoothly (convex curvature I *vs.* T). Despite the fact that the FM moment is partially supported by the external in-plane magnetic field, $H_{\rm pl}$, it undoubtedly seems to show a phase transition-like behavior at T_1. The expected spin structure including both transverse AF and FM ordering is tentatively sketched in Figure 1 at the lefthand side of the $H_1(T)$ line by tilted arrow symbols including their precession circles.

In order to understand these results let us recall the possible importance of off-diagonal exchange interaction between planar and axial spin components in $FeBr_2$ [6]. In our preliminary interpretation, solely based on magnetization measurements, we suggested the appearance of an disorder-order phase transition of the transverse spin-components when crossing the line $H_1(T)$ and entering the phase AF II. According to the neutron data, this assertion is still partially valid. While maximum transverse AF spin order is observed at $H_1(T)$, it decreases when entering the phase AF I. Conspicuously, in parallel with this decrease intraplanar FM ordering establishes phase transition-like as seen by the onset of additional (0, 0, −1) scattering intensity (Fig. 4). Obviously the in-plane spin components are tilted towards a common FM axis in the low-T phase AF I in a phase transition-like fashion. It is tempting to assume the appearance of weak transverse ferromagnetism, although experimental evidence for a sizeable FM component in the (0, 0, −1) scattering intensity in a purely axial magnetic field (not shown) is still lacking.

Weak ferromagnetism is often [14,15] attributed to the antisymmetric part of the off-diagonal exchange interactions terms of the form $\mathbf{d} \cdot [\mathbf{S}_i \times \mathbf{S}_j]$, where $\mathbf{S}_{i,j}$ are spins from different sublattices and $\mathbf{d}$ is a coupling vector, the size and direction of which depends on spin and spatial symmetry. However, as can easily be shown for the space group D^3_{3d} of $FeBr_2$, inversion symmetry is present between all spin pairs in- and out-of-plane. Hence, no Dzialoshinski-Moriya-type coupling is expected to occur.

One has then to check the relevance of symmetric off-diagonal exchange interactions, which are expected to occur in the trigonal point group of $FeBr_2$ [7]. Using symmetry arguments a straightforward analysis shows that off-diagonal exchange of the type $-J\,(S^x_0 S^z_1 + S^x_1 S^z_0)$ should exist for both in- and inter-plane bonds, *viz.*, $J = J_1(a,0,0)$, $J_2(a,a,0)$, $J_3(2a,0,0)$, $J'_1(a,0,c)$ and $J'_2(2a,0,c)$, where the subscripts 1, 2 and 3 denote nearest, next-nearest and third-nearest spin neighbors, respectively, while the argument describes the position of $\mathbf{S}_1$ with respect to that of $\mathbf{S}_0$, (0, 0, 0). However, owing to the threefold rotational symmetry their contributions vanish in case of a Néel-type ground state involving only two sublattices, *i.e.* $q_x = q_y = 0$ and $q_z = c^*/2$. This was already remarked by Mukamel for the nearest-neighbor in-plane exchange, $J = J_1(a,0,0)$ [7]. Unfortunately there is presently no hint at either a non-collinear or a modulated transverse spin structure in $FeBr_2$, which might activate the off-diagonal exchange and finally explain the appearance of a spontaneous transverse ferromagnetic moment below T_1. Here we tentatively propose that intraplanar secondary anisotropy will break the planar spin order into domains, similarly as observed on the oblique AF phase of the competing anisotropy system $Fe_{1-x}Co_xCl_2$ [16]. By virtue of domain wall-induced spin disorder the off-diagonal exchange may thus become active.

However, lacking both theoretical and experimental evidence of this moment for $H_{\rm pl} = 0$, we alternatively propose the above increase of the FM scattering

intensity (Fig. 4) to be due to a spin-flop like reorientation of the AF in-plane order parameter induced by $H_{\rm pl}$ at $T < T_1(H)$. Unfortunately this does not explain the existence of a phase transition in the absence of $H_{\rm pl}$ [5].

A similar intraplanar spin-flop at the phase line $H_1(T)$ was recently found by Pleimling [17] in computer simulations. He introduced a semi-classical Heisenberg model taking into account off-diagonal exchange interaction between intraplanar spins. Within this approach the axial and transverse spin-components are decoupled and two distinct transition temperatures, $T_{\rm c}$ and T_{xy}, are encountered. The latter temperature corresponds to T_1 in the experimental phase diagram. However, in disagreement with the experimental results (Figs. 4 and 5) destruction (instead of gradual thermal decrease) of the transverse AF order is observed when heating the system to above T_{xy}. Further, this model predicts a phase transition also for $H_{\rm ax} = 0$ at $T_{xy} < T_{\rm N}$, an assertion which still lacks confirmation.

Yet another description was suggested by Acharyya *et al.* [18]. They considered a weakly anisotropic Heisenberg system and succeeded in reproducing the transverse AF order parameter curves I (0, 0, $-1/2$) *vs.* T (Figs. 4 and 5) in terms of a spin-flop transition. It occurs at $T(H_1)$ and is driven by the applied axial field. This model suffers from the drawback that, in contrast with the experimental observation, any transverse AF ordering is lacking at low T in a sufficiently weak axial field H. Moreover, it is unable to explain the metamagnetic phase transition as observed in $FeBr_2$ below T(MCP) (Fig. 1).

It is clear that both the experimental data and the theoretical description of $FeBr_2$ are still far from being complete. The oblique nature of the AF phases throughout the phase diagram sheds new light onto the nature of the phase transition at $T_{\rm c}(H)$. Since it is characterized by a merger of two order parameters, $S_{\parallel}$ and $S_{\perp}$, referring to two different irreducible representations of the D^3_{3d} space group, a second-order phase transition seems to be excluded within Landau theory. Indeed, the observed [19] asymmetric critical behavior of the magnetic specific heat might hint at the appearance of either a weak first-order transition or of two unresolved successive second-order transitions.

Further, the peak-like behavior of the transverse AF order parameter at $H_1(T)$ and the gradual vanishing of this peak as $H \to 0$ are only poorly understood. In particular, the nature of the new order parameter characterizing the AF I phase is still unclear. As outlined above there is some evidence that symmetric off-diagonal spin coupling in conjunction with a modulated spin structure might eventually solve the puzzle. Here the existence of in-plane frustration due to competing interactions, $J_3/J_1 = -0.2$ [20], seems to be crucial. Additional need for a fully quantum mechanical treatment [17] is still an open question.

We would like to thank M. Acharyya, M. Pleimling and W. Selke for helpful discussions, H. Junge for the growth of some $FeBr_2$ crystals and the Deutsche Forschungsgemeinschaft (Graduiertenkolleg "Struktur und Dynamik heterogener Systeme") for financial support.

References

1. J.M. Kincaid, E.G.D. Cohen, Phys. Rep. C **22**, 57 (1975).
2. E. Stryjewski, N. Giordano, Adv. Phys. **26**, 487 (1977).
3. M.M.P. de Azevedo, Ch. Binek, J. Kushauer, W. Kleemann, D. Bertrand, J. Magn. Magn. Mater. **140–144**, 1557 (1995).
4. J. Pelloth, R.A. Brandt, S. Takele, M.M.P. de Azevedo, W. Kleemann, Ch. Binek, J. Kushauer, D. Bertrand, Phys. Rev. B **52**, 15372 (1995).
5. H. Aruga Katori, K. Katsumata, M. Katori, Phys. Rev. B **54**, R9620 (1996).
6. O. Petracic, Ch. Binek, W. Kleemann, U. Neuhausen, H. Lueken, Phys. Rev. B **57**, R11051 (1998).
7. D. Mukamel, Phys. Rev. Lett. **46**, 845 (1981).
8. K. Katsumata, H. Aruga Katori, S.M. Shapiro, G. Shirane, Phys. Rev. B **55**, 11466 (1997).
9. W. Selke, Z. Phys. B **101**, 145 (1996).
10. M. Pleimling, W. Selke, Phys. Rev. B **56**, 8855 (1997).
11. O. Petracic, Ch. Binek, W. Kleemann, *Proceedings SDHS'99 Duisburg* (World Scientific, Singapore, 2000) in print, `cond-mat/9906003`.
12. R.J. Birgeneau, G. Shirane, M. Blume, W.C. Koehler, Phys. Rev. Lett. **33**, 1098 (1974).
13. J.F. Dillon, E.Yi Chen, H.J. Guggenheim, Solid. State Commun. **16**, 371 (1975).
14. I. Dzialoshinski, J. Phys. Chem. Solids **4**, 241 (1958).
15. T. Moriya, Phys. Rev. **117**, 635 (1960).
16. W. Nitsche, W. Kleemann, Phys. Rev. B **36**, 8587 (1988).
17. M. Pleimling, Eur. Phys. J. B **10**, 465 (1999).
18. M. Acharyya, U. Nowak, K.D. Usadel, Phys. Rev. B **61**, 464 (2000).
19. M.C. Lanusse, P. Carrara, A.R. Fert, G. Mischler, J.P. Redoulès, J. Phys. France **33**, 429 (1972).
20. S. Pouget, Ph.D. Thesis, INSA Toulouse, France, 1993.